Advances in Water Resources 50 (2012) 55–61

Contents lists available at SciVerse ScienceDirect

Advances in Water Resources

journal homepage: www.elsevier.com/locate/advwatres

Surface soil water content spatial organization within irrigated and non-irrigated agricultural fields ☆

Michael H. Cosh [a,*], Steven R. Evett [b], Lynn McKee [a]

[a] USDA-ARS-Hydrology and Remote Sensing Laboratory, Beltsville, MD, USA
[b] USDA-ARS-Conservation and Production Research Laboratory, Bushland, TX, USA

ARTICLE INFO

Article history:
Available online 24 July 2012

Keywords:
Soil water content
Network analysis
Temporal stability

ABSTRACT

Understanding soil water content, θ, variability is important for monitoring and modeling of land surface processes as well as land and water management practices. With regards to in situ θ probes, it is sometimes assumed that a single local measurement can represent the larger domain, mostly for practical reasons. But there is a substantial amount of variability in θ at the field scale. As part of the Bushland Evapotranspiration and Agricultural Remote Sensing Experiment 2008 (BEAREX08), a high-density sensor network and intensive observational periods were developed to fully describe the θ conditions at the surface on the field scale, in support of the hydro-meteorological measurements being collected. A total of 20 θ stations were distributed over an irrigated and a non-irrigated field (~10 ha each) and high-density (~every 5 cm) transects were measured for a high-detailed record. The network was able to provide large scale estimates of θ with an accuracy (root mean square error, RMSE) of 0.035 m^3/m^3. The network was temporally stable with the exception being immediately during and after irrigation events. Irrigation caused significant increases in coefficients of variation due to the length of time (8–12 h) necessary to irrigate the entire field. The spatial distribution of surface θ was significantly affected by the row structure of the cotton plants, which was North–South in the field where transect measurements were made with a row spacing of 76 cm. At scales <35 cm (approximately half the row spacing), the distribution was correlated in the East–West direction. For scales larger than 35 cm in the East–West direction the correlation decreased, but was still present. In the North–South direction this discontinuity was not present, and θ followed a power law distribution.

Published by Elsevier Ltd.

1. Introduction

Remote sensing technology exists that can estimate surface soil water content, θ, on large scales [22], but the validation of those technologies requires ground-truth at field and larger scales. Large scale in situ networks exist, such as the Soil Climate Analysis Network [25] and the Climate Reference Network [23], but the individual stations consist of localized measurements. Most in situ sensors only measure at small scales. Many current commercial sensors respond to soil permittivity of a small volume of soil immediately surrounding the sensor [8], often with a length scale less than 10 cm. For validation studies, which use in situ data, it is necessary to examine methodologies for scaling these small scale (local) in situ data to large remote sensing footprints. Understanding the variability of θ at the surface, impacts not only satellite validation programs, but also field experimenters who must provide accurate field estimates, and modelers who must understand distributions of θ.

An earlier study of the spatial organization of θ was conducted by Rodriguez-Iturbe et al. [24] who used remote sensing data from the Washita '92 experiment [15]. They used aggregation analysis of 200-m aircraft remote sensing pixels along with ground sampling at a 30-m resolution to determine that θ followed a power law distribution at the field scale. Cosh and Brutsaert [5] continued this analysis using semivariogram analysis and determined that θ was stationary within the field scale (~800 m) for this data set. One of the first field based studies into the distribution and scaling of θ from local to field scales was conducted by Famiglietti et al. [12]. This study collected high-density field samples of θ during a remote sensing field campaign and analyzed how θ variability changed depending on the scale. This study used descriptive statistics to determine how the distribution of θ varied in response to precipitation events and the subsequent dry-down. This was extended by Mohanty et al. [21] by using variogram analysis to determine the characteristic length scales of θ based on the

☆ USDA is an equal opportunity provider and employer. The mention of trade names of commercial products in this article is solely for the purpose of providing specific information on and does not imply recommendation on or endorsement by the USDA.

* Corresponding author.
E-mail address: Michael.Cosh@ars.usda.gov (M.H. Cosh).

0309-1708/$ - see front matter Published by Elsevier Ltd.
http://dx.doi.org/10.1016/j.advwatres.2012.07.009

sampling conducted during the Southern Great Plains Hydrology Experiment in 1997 (SGP97) [16]. These studies brought the understanding of θ variability down to the meter scale, though most of the land cover types were pasture or harvested winter wheat, which generally exhibit isotropic behavior. There was little to no row structure in those agricultural fields, which ignores a large portion of agricultural land surface conditions.

These studies were limited by the datasets collected and were only able to study θ spatially on a scale as small as 1 m [1,12]. The present study was designed to collect high-resolution data under various θ conditions to determine the spatial distribution of θ from the measurement scale to the field scale for purposes of informing large-scale estimation for remote sensing validation. To do this, it is necessary to collect dense samples at the scale of the instrument of study. In the case of most in situ networks, the instrument scale is in the range of 5–30 cm. This study was conducted in coordination with an intensive aircraft and meteorological flux measurement experiment at the USDA-Agricultural Research Service Laboratory in Bushland, TX. Various geostatistical and statistical analyses were applied to the data collected, to explore the distribution of θ on this fine scale. The results of this study will inform remote sensing validation campaigns on methodologies for field scale estimation of surface θ, by helping to define characteristic length scales and spatial distribution characteristics.

2. Experiment design

The Bushland Evapotranspiration and Agricultural Remote Sensing Experiment 2008 (BEAREX08) was conducted in the summer of 2008 near Bushland, Texas at the USDA-ARS Conservation & Production Research Laboratory [11]. The BEAREX08 experiment was developed to study at sub-field, field and watershed scales how evaporation can be estimated and modeled using a variety of techniques including aircraft thermal remote sensing, energy flux measurements and in situ instrumentation. A key component of this experiment was the monitoring and estimation of θ at the land surface. The experimental domain for θ measurements was located within a 450 m by 450 m cotton field, which had wheeled sprinkler irrigation that operated on the eastern half of the field. Intensive aircraft campaigns were organized to measure the energy and surface fluxes over the domain to coincide with numerous ground-based energy flux measurements [11].

Within these two experimental fields, referred to as WET (irrigated) and DRY (non-irrigated), there were 20 θ sensors installed in an X-pattern in each field (Fig. 1). These mini-stations consisted of a Hydra Probe (Stevens Water Monitoring Systems, Inc., Portland, OR, USA) installed horizontally and sensing θ across a depth of 3–7 cm approximately. The reported accuracy of these sensors in the Pullman soil at the study site is ±0.015 m^3/m^3, but with inter-sensor variability of up to 0.07 m^3/m^3 [3]. This probe installation is similar to the surface sensing scheme of the Soil Climate Analysis Network (SCAN) and Climate Reference Network (CRN) stations in the U.S. [25,13]. This depth of installation is frequently related to the 0–5 cm average volumetric θ for purposes of remote sensing validation [17].

As part of the water management program, the DRY cotton field was irrigated a total of three times (to establish the crop) and the WET cotton field was irrigated 17 times. The experiment started with the planting of cotton on May 21, 2008 and the data time series began on June 5, 2008, when equipment was installed. The time series was sustained until mid November. There was substantial vegetation growth as a result of above normal precipitation beginning in mid August and this resulted in the time series becoming intermittent in August as the foliage began to obscure the solar panels, interrupting battery recharging.

3. Methods of experimentation

In addition to the static in situ network, manual sampling collected high-density θ estimates with a dielectric probe (Theta Probe ML-2, Delta-T Ltd., United Kingdom). The sensing elements of the probe measure approximately 3 cm in diameter and 6 cm in length. The measurement volume is approximately 5 cm in diameter. Several transects of 900–1000 sampling points were collected in various directions, each sample separated by 5 cm, providing a near spatially continuous transect. The transect was sampled over the course of 1 h. This length of time would not result in a significant loss of θ during the time period of sampling.

For purposes of validating the network for the overall BEAREX08 study period, a method for large-scale sampling was established. The in situ network average for each field was calculated using the calibration equations developed by Evett et al. [9], for the local soils in the field of study. This calibrated network average was compared to the large-scale θ (as determined by gravimetrically calibrated Theta probe sampling). Five days of intensive sampling (>60 samples) with the Theta probe were conducted for each field (WET and DRY).

4. Experimental analysis

Four different methods of investigation were used to explore the spatial data collected during BEAREX08. Initially, the quality of the network was evaluated using the root mean square deviation of the network average as compared to large-scale θ measurements using the thermogravimetric method [6]. The thermogravimetric method was established as the primary requirement for ground truth of θ estimates by NASA and ESA for their missions [7,19,22]. Temporal stability analysis was used to investigate the persistence of the θ patterns in the field and what affects these patterns. Semivariogram analysis was used to explore the characteristic length scales involved at the sampling scale in the landscape. Finally, aggregation analysis was used to consider if the power law distribution described surface θ and at what scales.

4.1. Temporal stability

Once it was determined that the network could accurately represent the domain, we sought to determine if the θ pattern was persistent in time, or temporally stable. Demonstrated by Vachaud et al. [26], temporal stability analysis is a useful tool for analyzing the spatial distribution of θ and for providing quality assurance on a sensing network. The basis of the analysis is the calculation of the mean relative difference function. The mean relative difference, $\overline{\delta}_1$, is defined as

$$\overline{\delta}_1 = \frac{1}{t}\sum_{j=1}^{t}\frac{S_{i,j} - \overline{S}_j}{\overline{S}_j} \tag{1}$$

where $S_{i,j}$ is the jth sample at the ith site of n sites within the field and $\overline{S}_j$ is the computed average among all sites for a given date and time, j (j = 1 to t). The mean relative difference compares the value at a particular site to the average over the area of study at that instance in time. It determines if a location is consistently greater or less than the mean and how variable that relationship is as determined by the standard deviation of the relative differences (SDRD), defined as

$$\sigma(\delta)_i^2 = \sqrt{\frac{1}{t-1}\sum_{j=1}^{t}\left(\frac{S_{i,j} - \overline{S}_j}{\overline{S}_j} - \overline{\delta}_i\right)^2} \tag{2}$$

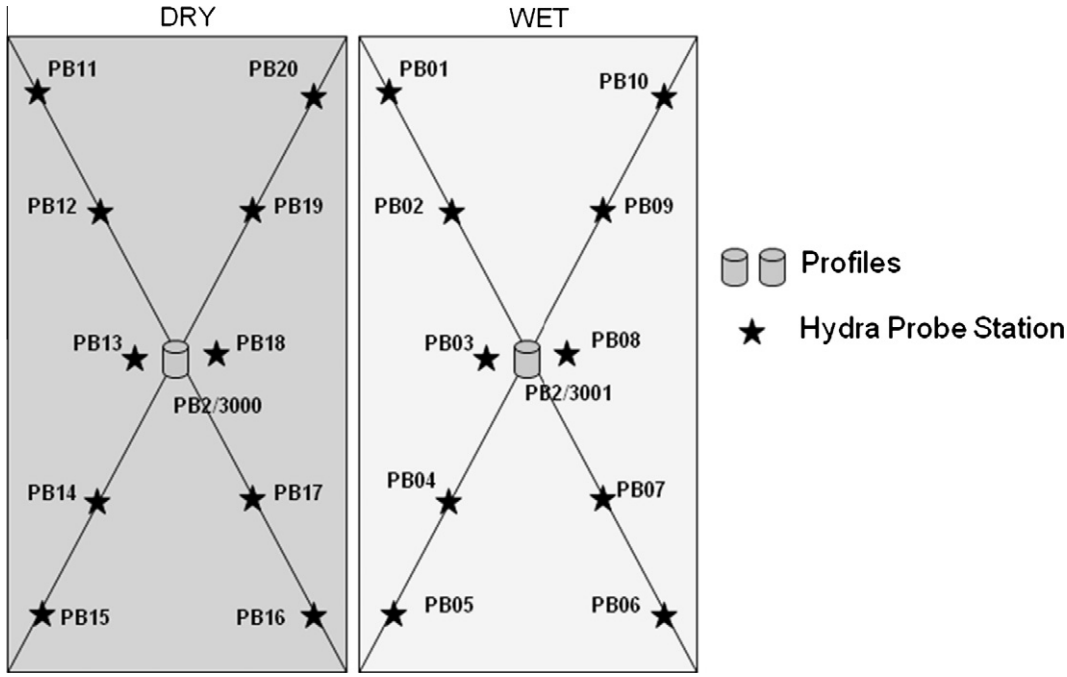

Fig. 1. Installation diagram for the BEAREX08 soybean field. The label "Hyda Probe Station" indicates locations of Hydra Probe installation horizontally centered at 5-cm depth. The label "Profiles" indicates locations where Hydra Probe sensors were installed centered at the 5-cm depth and at deeper depths to 40 cm.

A location is temporally stable if it has a low SDRD (for this study, approximately less than 0.75 m^3/m^3), such that there is a consistent, though potentially biased relationship between the site and the overall average. A site is representative of the large-scale average if its $\bar{\delta}_i$ is near zero. A large $\bar{\delta}_i$ (positive or negative) is a potentially correctable problem, whereas a large SDRD is not for the purposes of extrapolation. It is possible to detect anomalous locations with this analysis, by assessing the SDRD in relation to the other SDRD values, and examining the dynamic ranges of the θ estimates.

4.2. Semivariogram analysis

The semivariogram is a common geostatistical tool, which has been used to study θ variability [2,5,18]. The semivariogram, $\gamma(h)$, is the expected value of the square of the increments of a function, $Z(x)$, and is defined as

$$\gamma(h) = \frac{1}{2N_p}\sum_{i}^{N_p}[Z(x_i) - Z(x_{i+h})]^2 \quad (3)$$

where h is the separation distance for location x_i and x_{i+h} [18]. The semivariogram is often normalized by the variance and modeled to summarize the underlying function $Z(x)$. For this study, a power law distribution was hypothesized [20], and characterized by

$$\gamma(h) \sim h^{2Ha}$$

where Ha is the Hausdorff exponent. As the exponent approaches zero, the distribution becomes more homogeneous and spatially stationary. The distance at which the slope becomes zero is the correlation length.

4.3. Aggregation analysis

To study the effect of sampling scale on mean and variance estimation, aggregation analysis was conducted. Following the procedures established by Rodriguez-Iturbe et al. [24] and Hu et al. [14], the variance was calculated for a sampling transect at the sampling resolution. Next, the data series was aggregated to a lower resolution and the variance was recalculated. The process was repeated and the results plotted as variance versus the resampled resolution. The smallest scale in this study was 5 cm and analysis was conducted to 1 m. How the variance changed with sampling scale provided insight into how θ was organized spatially. Previous studies have observed a power law decay of the variance with sampling scale, but none have analyzed data down to the scales in this study.

5. Results of network analysis

The first set of analyses was conducted on the Hydra Probe Network, which was installed to support activities at BEAREX08. Evett et al. [9] developed a calibration for the probes used in the network and this calibration was applied to this dataset. Five days of intensive thermogravimetric θ sampling were conducted throughout the summer of 2008 to provide a more thorough estimate of the large scale mean of θ. The RMSE for the network average as compared with the large scale field average was 0.035 m^3/m^3. Fig. 2 is a time series plot of the field averages along with the precipitation and irrigation patterns. The large-scale physical sampling averages are also plotted. It was determined that the network average could not be practically improved upon, and further calibration of the Hydra Probe network was unnecessary for the purposes of this experiment. Station 3 (in the WET field) was not included in this study, because of it contained a faulty sensor, which resulted in an inconsistent data record. When computing the errors on the field basis, the WET field had an RMSE of 0.054 m^3/m^3 and the DRY field had an RMSE of 0.017 m^3/m^3. The larger errors for the WET field were investigated further below.

It became evident that there was a very different θ distribution between the WET field and the DRY field, depending on the event considered. This difference was evidenced by a plot of the time series of the coefficients of variation for each network (Fig. 3). For precipitation events, in both fields CV increased slightly, but for irrigation events, the WET field CV dramatically increased in

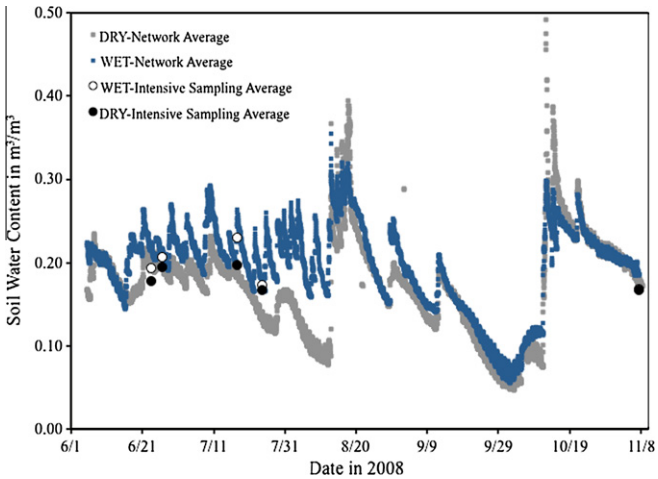

Fig. 2. Time series of the volumetric soil water content averages for the DRY and WET fields.

comparison with the DRY field. This was a result of the type of irrigation used in the study. The wheeled sprinkler assembly moved slowly across the field, taking between 8 and 12 h to cover the entire surface depending on the depth of water applied. This caused the surface to have a large degree of variability in the 24 h after irrigation.

A temporal stability analysis was conducted on each of the networks (WET and DRY) separately, and it was observed that each network demonstrated temporally stable characteristics (Fig. 4). At least qualitatively, the θ patterns were persistent, indicating that some locations in the network did and some did not represent the overall mean θ. The variation in mean relative difference was approximately three times larger in the DRY field than in the WET field. This result agrees with that of Evett et al. [10] who found that variability was larger in drier soils for the dielectric sensors that they studied. To further assess the spatial characteristics of the field, semivariogram analysis must be employed.

5.1. Results of high density sampling analysis

To study the measurement scale, a series of high-density sampling transects were conducted with Theta Probes. Factory calibration for the Theta Probe yielded an RMSE of 0.056 m^3/m^3, but after gravimetric calibration, the RMSE was reduced to 0.024 m^3/m^3, following Cosh et al. [4]. Fig. 5 shows a comparison of the uncalibrated and calibrated Theta Probe measurements compared to gravimetrically-based volumetric θ.

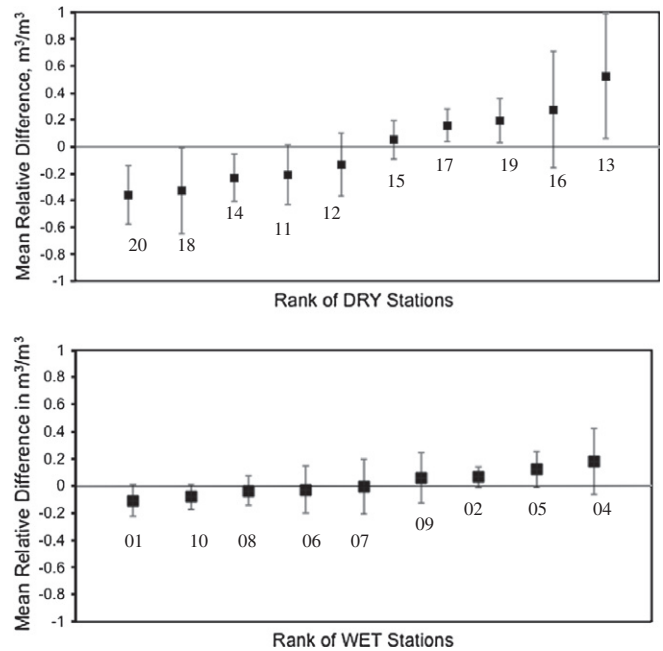

Fig. 4. Mean relative difference plots for the DRY and WET networks.

A total of six transects were available for study after quality control eliminated several of the other transects collected during the experimental periods. Table 1 contains a description of the transects and their characteristics. East–West transects crossed over the cotton plant rows and North–South transects went along the row, approximately ¼ of the distance between plant rows.

5.2. Semivariogram results

Semivariograms are presented in Fig. 6 and have been scaled by the variance of each transect to account for differences between sampling dates. The figure is presented in log–log form, which reveals how the distribution obeys a power-law by the degree to which it follows a straight line. The cotton plants were arranged in North–South rows and in the WET field, there was significant microtopography, such that the plant rows were nearly 20 cm higher in elevation than the interrow surface. The row spacing was approximately 76 cm, and this was evident in the East–West

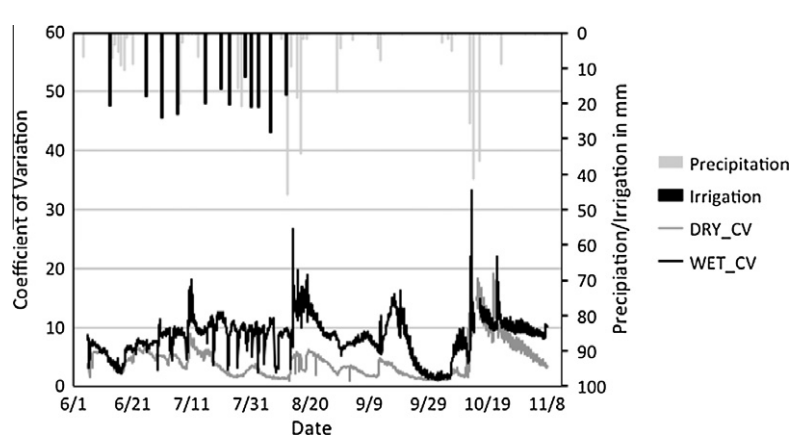

Fig. 3. Time series of coefficients of variation with precipitation and irrigation plotted.

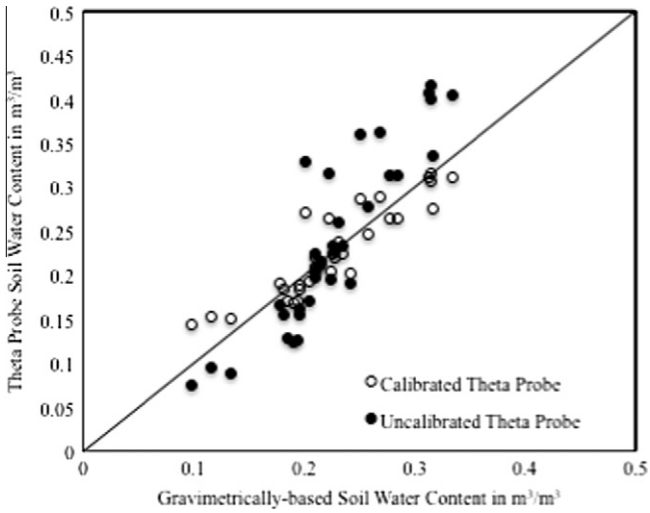

Fig. 5. Comparison of soil water content estimates for factory (uncalibrated) and calibrated Theta Probe functions. RMSE for uncalibrated is 0.056 m^3/m^3 and for calibrated is 0.024 m^3/m^3.

Table 1
Sampling characteristics of the high density transects. Aggregation coefficient refers to the exponents of the relationship on a log–log plot.

Field	Date	Direction	Number of points	Aggregation coefficients
WET	6/27/08	EW	907	−0.387/−0.803
WET	6/27/08	NS	900	−0.247
WET	7/24/08	NS	1048	−0.267
WET	7/27/08	EW	1048	−0.455/−0.752
DRY	7/23/08	EW	1048	−0.351/−0.940
DRY	7/23/08	NS	1048[a]	−0.402

[a] A transect with quality control measures employed.

semivariograms, which exhibited a characteristic length scale of approximately 35 cm and reached a sill after this length. Transects in the North–South direction did not exhibit this same length scale and also exhibited non-stationarity.

5.3. Aggregation results

The same characteristic length scale was observed in the East–West direction when examining the results of the aggregation analysis. Fig. 7 shows how the variance changes as the resolution of the sampling is reduced from the maximum density of 5 cm to 1 m for sampling on 27 June 2008 in both the East–West and North–South directions in the WET field. On a log–log plot, at approximately 35 cm, there was a break in the slope of the East–West transect. The slope break was not evident in the analysis for the North–South transect, which is along the row direction. Furthermore, the two variances became approximately equal at 60 cm, which was relatively close to the row spacing of 76 cm. These slopes are referred to as the aggregation coefficients and are the exponents on the power-law plots and are shown in Table 1. Similar results were found for the aggregation variances of the other transects. For the East–West transect, the power law coefficient was approximately −1 for distances greater than 0 cm to 1 m for this date, which is indicative of a spatially independent identically distributed process. For the other East–West transects, this coefficient ranged between −0.4 and −1.0. For distances between 5 cm and 35 cm in the East–West transects, the coefficient ranged between −0.2 and −0.4, and this was similar for the North–South transects. For perspective, a coefficient of 0 is a completely correlated variable and −1 indicates a completely random process. For the majority of transects in this study, θ followed a power law distribution indicating spatial correlation for two distinct scales.

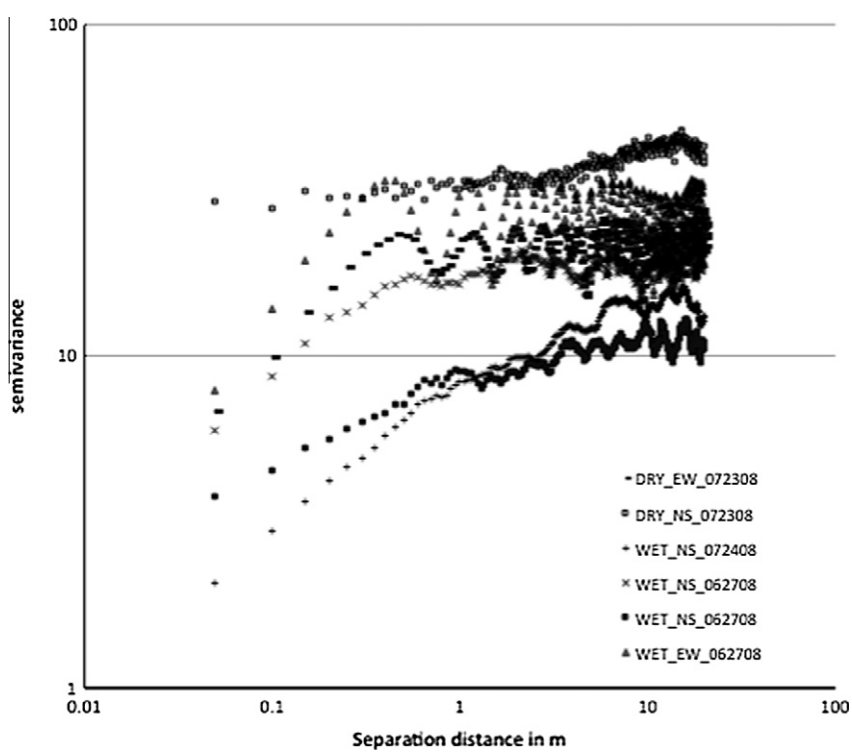

Fig. 6. Semivariograms of the six sampling transects.

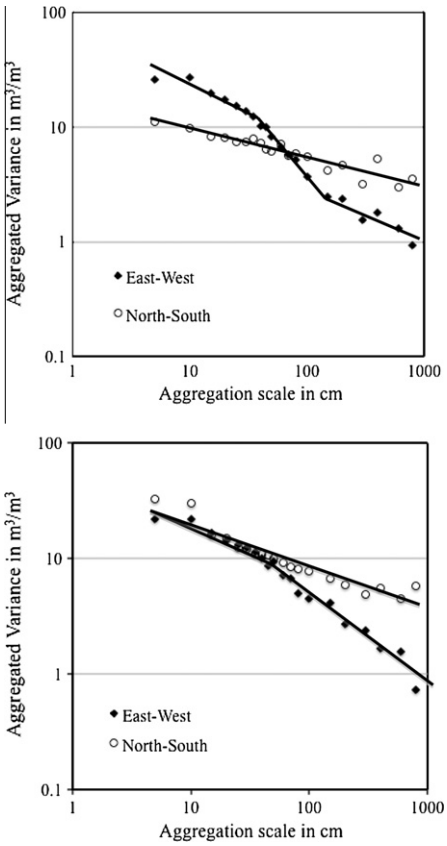

Fig. 7. The aggregation variance cascade with increasing aggregation scale for an east west transect for the WET field on 6/27/08 and the DRY field on 7/23/08, respectively.

6. Conclusions

In review, the stability and distribution of θ was determined from the measurement scale to the field scale for the BEAREX08 study domain. The θ patterns in the agricultural fields were persistent during the study period, as demonstrated by the temporal stability analysis. This shows that it is possible to have a stable soil moisture pattern within an agricultural field, which will have an impact on the ability to improve efficiencies in field sampling of θ. The variability, as demonstrated by the coefficient of variation, increased in the irrigated field after irrigation because of the slow temporal variations in water content input. Irrigation was a long process, taking up to 12 h, while precipitation was relatively quick, providing a more uniform input. The ability of the in situ network to accurately represent the surface was not impacted because there was a spatial distribution of sensors across the field. The variability of water content across the surface, however, was strongly impacted during irrigation events. It is concluded that a large number of θ in situ stations are necessary to monitor irrigated fields if the intent is to capture the spatial domain of the field under the irrigation equipment during and for a period of time after the irrigation. In this study, the period of time after an irrigation, during which spatial variation in water content remained strong, was approximately three times the duration of the irrigation event.

Using semivariogram analysis on the high density dataset, it was determined there was a characteristic length scale of approximately 35 cm across the planting rows, which coincided with about one half the row spacing. This finding was supported by aggregation analysis, which also found that within this length scale θ followed a power law distribution with a coefficient of approximately 0.25. This finding is in agreement with previous studies [14]. Beyond this length scale, the correlation decreased, but maintained some amount of correlation more than a random process. This length scale is critical to large-scale sampling designs often used by remote sensing campaigns to characterize the land surface. It also sets the minimum separation distance for small impedance probes ($\sim$5 cm) such as those used in this study and in large scale in situ networks. This will impact validation campaigns, which often make assumptions of how in situ sensors represent large-scale averages. Modelers will also benefit from the increased understanding of the power law distribution of surface θ. These results, however, may be somewhat soil and farming system dependent, so should be combined with those from previous and future studies in assessing sampling needs for validation campaigns.

References

[1] Brocca L, Melone F, Moramarco T, Morbidelli R. Spatial-temporal variability of soil moisture and its estimation across scales. Water Resour Res 2010;46:W02516. http://dx.doi.org/10.1029/2009WR008016.
[2] Brocca L, Morbidelli R, Melone F, Moramarco T. Soil moisture spatial variability in experimental areas of central Italy. J Hydrol 2007;333:356–73.
[3] Chávez JL, Evett SR. Using soil water sensors to improve irrigation management. In: Proceedings 24th annual central plains irrigation conference. Colby, Kansas; 2012. 21–22 February 2012.
[4] Cosh MH, Jackson TJ, Bindlish R, Famiglietti JS, Ryu Dongryeol. Calibration of an impedance probe for estimation of surface soil water content over large regions. J Hydrol 2005;311(1–4):49.
[5] Cosh MH, Brutsaert W. Aspects of soil moisture variability in the Washita '92 study region. J Geophys Res 1999;104(D16):19751–7.
[6] Dane JH, Topp GC. Methods of soil analysis, part 4, physical methods. Madison, WI, USA: Soil Science Society of America; 2002.
[7] Entekhabi D, Njoku EG, O'Neill PE, Kellogg KH, Crow WT, Edelstein WN, et al. The soil moisture active passive (SMAP) mission. Proc IEEE 2010;98(5):704–16.
[8] Evett SR, Parkin GW. Advances in soil water content sensing: the continuing maturation of technology and theory. Vadose Zone J 2005;4:986–91. http://dx.doi.org/10.2136/vzj2005.0099.
[9] Evett SR, Tolk JA, Howell TA. TDR laboratory calibration in travel time, bulk electrical conductivity, and effective frequency. Vadose Zone J 2005;4:1020–9.
[10] Evett SR, Scwhartz RC, Tolk JA, Howell TA. Soil profile water content determination: spatiotemporal variability of electromagnetic and neutron probe sensors in access tubes. Vadose Zone J 2009;8(4):926–41.
[11] Evett SR, Kustas WP, Gowda PH, Anderson MC, Prueger JH, Howell TA. Overview of the Bushland evapotranspiration and agricultural remote sensing experiment 2008 (BEAREX08): a field experiment evaluating methods for quantifying ET at multiple scales. Adv Water Resour 2012;50:4–19.
[12] Famiglietti JS, Devereaux JA, Laymon CA, Tsegaye T, Houser PR, Jackson TJ, et al. Ground-based investigation of soil moisture variability within remote sensing footprints during the Southern Great Plains 1997 (SGP97) hydrology experiment. Water Resour Res 1999;35(6):1839–51.
[13] Heim R. New network to monitor climate change. Eos Trans Amer Geophys Union 2001;82:143.
[14] Hu Z, Islam S, Cheng Y. Statistical characterization of remotely sensed soil moisture images. Remote Sens Environ 1997;61:310–8.
[15] Jackson TJ, Le Vine DM, Swift CT, Schmugge TJ, Schiebe FR. Large area mapping of soil moisture using the ESTAR passive microwave radiometer in Washita '92. Remote Sens Environ 1995;54(1):27–37.
[16] Jackson TJ, Le Vine DM, Hsu AY, Oldak A, Starks PJ, Swift CT, et al. Soil moisture mapping at regional scales using microwave radiometry: the Southern Great Plains hydrology experiment. IEEE Trans Geosci Remote Sens 1999;37(5):2136–51.
[17] Jackson TJ, Cosh MH, Bindlish R, Starks PJ, Bosch DD, Seyfried MS, et al. Validation of advanced microwave scanning radiometer soil moisture products. IEEE Trans Geosci Remote Sens 2010;48:4256–72.
[18] Journel AG, Huijbregts CJ. Mining geostatistics. London, UK: Academic Press; 1978.
[19] Kerr YH, Waldteufel P, Wigneron JP, Delwart S, Cabot F, Boutin J, et al. The SMOS Mission: new tool for monitoring key elements of the global water cycle. Proc IEEE 2010;98(5):666–87.
[20] Malamud BD, Turcotte DL. Self-affine time series: I. Generation and analyses. Adv Geophys 1999;40:1–90.
[21] Mohanty BP, Famiglietti JS, Skaggs TH. Evolution of soil moisture spatial structure in a mixed vegetation pixel during the Southern Great Plains 1997 (SGP97) hydrology experiment. Water Resour Res 2000;36(12):3675–86.
[22] Njoku EG, Jackson TJ, Lakshmi V, Chan TK, Nghiem SV. Soil moisture retrieval from AMSR-E. IEEE Trans Geosci Remote Sens 2003;41:215–29.
[23] Palecki MA, Groisman PYa. Observing climate at high elevations using United States climate reference network approaches. J Hydromet 2011;12:1137–43. http://dx.doi.org/10.1175/2011JHM1335.

[24] Rodriguez-Iturbe I, Vogel GK, Rigon R, Entekhabi D, Castelli F, Rinaldo A. On the spatial organization of soil moisture fields. Geophys Res Lett 1995;22(20):2757–60.
[25] Schaefer GL, Cosh MH, Jackson TJ. The USDA natural resources conservation service soil climate analysis network (SCAN). J Ocean Atmos Technol 2007;24:2073–7.
[26] Vachaud G, Passerat De Silans A, Balabanis P, Vauclin M. Temporal stability of spatially measured soil water probability density function. Soil Sci Soc Amer J 1985;49:822–8.